PROCEEDINGS OF SPIE

SPIEDigitalLibrary.org/conference-proceedings-of-spie

3-D multitask deep neural networks for collateral imaging from dynamic susceptibility contrast-enhanced magnetic resonance perfusion

Le, Hoang Long, Jeon, Yejin, Roh, Hong Gee, Kim, Hyun Jeong, Kwak, Jin Tae

Hoang Long Le, Yejin Jeon, Hong Gee Roh, Hyun Jeong Kim, Jin Tae Kwak, "3-D multitask deep neural networks for collateral imaging from dynamic susceptibility contrast-enhanced magnetic resonance perfusion," Proc. SPIE 11597, Medical Imaging 2021: Computer-Aided Diagnosis, 1159721 (15 February 2021); doi: 10.1117/12.2581011

SPIE.

Event: SPIE Medical Imaging, 2021, Online Only

3-D Multitask Deep Neural Networks for Collateral Imaging from Dynamic Susceptibility Contrast-enhanced Magnetic Resonance Perfusion

Hoang Long Le[a], Yejin Jeon[b], Hong Gee Roh[c], Hyun Jeong Kim[d], Jin Tae Kwak*[e]
[a]Department of Computer Science and Engineering, Sejong University, Seoul, Korea 05006
[b]Division of Mechanical and Biomedical Engineering, Ewha Womans University, Seoul, Korea 03760
[c]Konkuk University Medical Center, Seoul, Korea 05029
[d]Daejeon St. Mary's Hospital, Catholic University, Daejeon, Korea 34943
[e]School of Electrical Engineering, Korea University, Seoul, Korea 02841

ABSTRACT

Acute ischemic stroke (AIS) is not only a common cause of disability but also a leading cause of mortality worldwide. Recent studies have shown that the collateral status could play a vital role in assessing AIS and determining the treatment options for the patients. Herein, we propose a joint regression and ordinal learning approach for AIS, built upon 3-D deep convolutional neural networks, that facilitates an automated and objective collateral imaging from dynamic susceptibility contrast-enhanced magnetic resonance perfusion (DSC-MRP). DSC-MRP images of 159 AIS subjects and 186 healthy subjects are employed to evaluate the proposed approach. The collateral status is manually assessed in arterial, capillary, early and late venous, and delay phases and served as the ground truth. The proposed method, on average, obtained 0.901 squared correlation coefficient, 0.063 mean absolute error, 0.945 Tanimoto measure, and 0.933 structural similarity index. The quantitative results between AIS and healthy subjects are comparable. Overall, the experimental results suggest that the proposed network could aid in automating the evaluation of collateral status and enhancing the quality and yield of diagnosis of AIS.

Keywords: Deep learning, Acute ischemic stroke, Magnetic resonance imaging, Collateral imaging, Multitask learning, Ordinal regression

1. INTRODUCTION

Acute ischemic stroke (AIS) is one of the lethal diseases worldwide, reducing mobility as well as lowering the quality of life of the patients [1]. Endovascular recanalization therapy has shown to be an effective manner of AIS treatment. However, a substantial portion of the patient population does not benefit from the treatment. Only those with the good collateral status can positively adapt to the treatment whereas patients with the poor collateral status are subject to hemorrhagic complications and poor recanalization rates [2] [3] [4] . To evaluate patients' collateral status, several approaches of collateral imaging have been proposed, including single-phase and multi-phase computer tomography angiography (CTA) [5] [6], dynamic susceptibility contrast-enhanced magnetic resonance perfusion (DSC-MRP) [7], dynamic contrast-enhanced magnetic resonance angiography [8] [9], and arterial spin labeling imaging[10]. Many of such methods rely on a semi-automated and sub-optimal assessment of arterial and/or venous signals, questioning on the reproducibility and accuracy of collateral imaging. Therefore, an automated, objective, and robust method that can assess the collateral status of the patients could facilitate an improved diagnosis and treatment of AIS in clinics.

In recent years, deep learning [11] has emerged as a powerful tool for processing and analyzing a massive amount of data as well as discovering intrinsic patterns and features in many applications. Among various deep learning approaches, a deep convolution neural network (CNN) has been successfully applied to several tasks in medical image analysis, including

*corresponding author: jkwak@korea.ac.kr; phone 82 2 6935-2492; fax 82 2 3408-4321; kwaklab.net

Medical Imaging 2021: Computer-Aided Diagnosis, edited by Maciej A. Mazurowski, Karen Drukker, Proc. of SPIE Vol. 11597, 1159721 · © 2021 SPIE
CCC code: 1605-7422/21/$21 · doi: 10.1117/12.2581011

object detection and segmentation, image registration, and image enhancement in pathology and radiology images [12] [13] [14]. An approach of CNN, in particular, has shown to be effective in analyzing

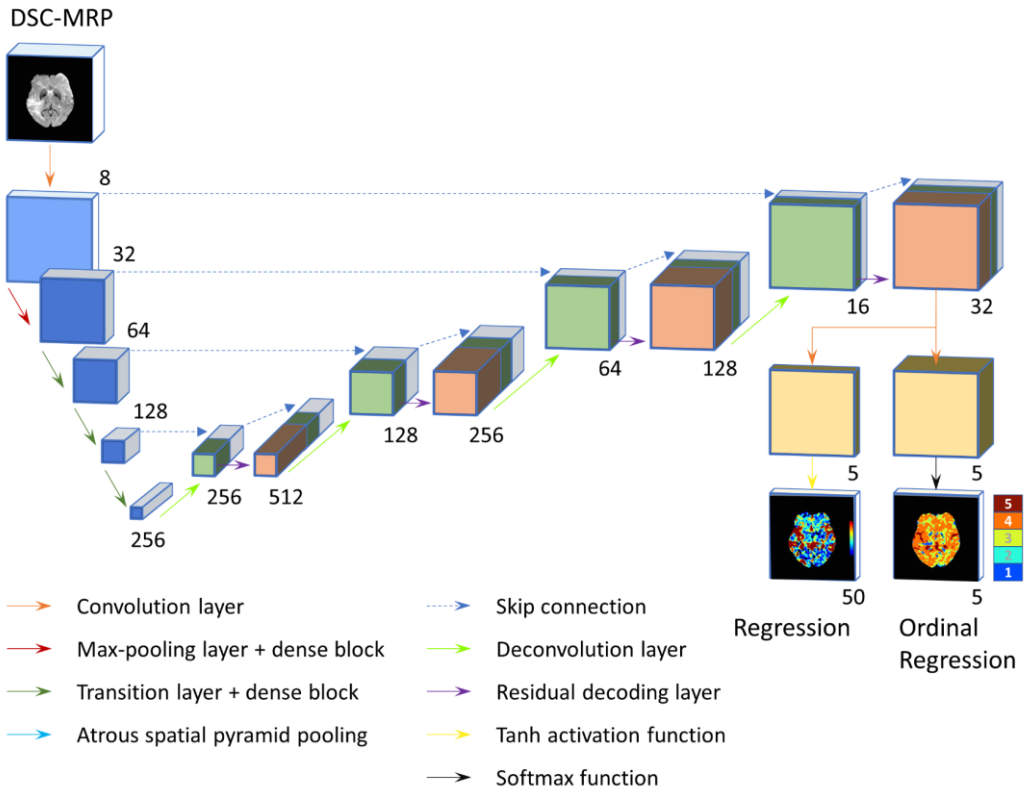

Figure 1. Network Architecture. The number indicates the number of feature maps.

brain magnetic resonance imaging (MRI). For instance, a deep voxelwise residual network was proposed for the segmentation of brain structures in MRI [15]. A fully convolutional network was combined with conditional random fields to conduct brain tumor segmentation in MRI [16]. A 3D CNN was adopted to process multi-modal MRIs and to predict a long or short overall survival time [17]. Moreover, a CNN has been employed to analyze patients with stroke. For example, a CNN was utilized to conduct an automated acute ischemic lesion segmentation in DWI [18]. Combing a U-Net structure and a gated recurrent unit layer, the prediction of stroke lesion outcome was performed using multi-parametric MRIs and clinical information [19]. In [20], an attention-gated U-Net was adopted to predict the final ischemic stroke lesions using multi-parametric MRIs. In [21], a 3-D deep regression neural network (3D-DRNN) was proposed to generate collateral images in DSC-MRP.

Among recent advances in deep learning, multi-task learning [22] has demonstrated its outstanding performance in improving the prediction power of a CNN. Multi-task learning is an approach that can simultaneously learn a collection of related tasks. By utilizing the shared representations among the related tasks, multi-task learning could reduce the computational cost and improve the generalizability of the model. In medical image analysis, the segmentation and classification tasks are often framed as a multi-task learning problem. For instance, the segmentation and classification of breast tissues were jointly conducted in biopsy images [23]. In [24], a multi-task learning CNN approach was proposed for the skin lesion segmentation and classification. The multi-task learning CNN includes three branches – one branch for the segmentation of skin lesions and two branches for the classification of skin lesions into melanoma, nevus, and seborrheic keratosis.

In this paper, we propose a 3-D multi-task deep regression neural network (3D-MDRNN) (Fig. 1) that can process and analyze 4-D DSC-MRP images for AIS assessment. The network utilizes 3-D convolutions to incorporate 3-D spatial information and performs both regression and ordinal regression, i.e., multi-task learning, to improve the overall performance of collateral imaging. As for the regression problem, the proposed approach aims to predict the voxel intensity of collateral imaging, which is in a range [-1, 1]. Applying spacing-increasing strategy (SID), we recast the regression problem as the ordinal regression problem by converting the continuous voxel intensities into discrete values. The model performance is evaluated via squared Pearson correlation coefficient (R-Squared), mean absolute error (MAE), Tanimoto measure (TM) [25], and structural similarity index (SSIM) [26]. The experimental results suggest that the proposed 3D-MDRNN could facilitate an automated, objective, and accurate collateral imaging for AIS.

2. METHODS

2.1 Dataset

This study includes 345 consecutive subjects collected from two university medical centers from November 2015 to September 2018. All participants gave informed consent. 345 subjects are divided into a training set, a validation set, and a test set. The training set contains 110 healthy and 95 AIS subjects (from November 2015 to August 2017). The validation set consists of 40 healthy and 24 AIS subjects (from September 2017 to December 2017). The test set comprises 51 healthy and 25 AIS subjects (from January 2018 to September 2018).

Given DSC-MRP of each subject, experienced neuro-radiologists generate the ground truth collateral imaging using in-house MATLAB-based software. Using the software, the neuro-radiologists select regions of interests (ROIs) on the normal side middle cerebral artery (MCA) and the superior sagittal sinus (SSS), examine arterial and venous signal intensity-time curves, and divide the curves into five phases, including (1) arterial phase (Art), (2) capillary phase (Cap), (3) early venous phase (Even), (4) late venous phase (LVen), and (5) delay phase (Del). By summarizing the signal intensity of DSC-MRP per phase, a collateral map is obtained. The detailed explanation of the procedure is available in [8].

2.2 Pre-processing

DSC-MRP undergoes a series of processing steps to identify the brain structure, i.e., a brain mask, in DSC-MRP and to reduce the computational cost. To build a brain mask, DSC-MRP images are summed up, 0-1 normalized, and thresholded at 0.1. Afterwards, closing, erosion, and dilation morphological operations are utilized to obtain a smooth and clean brain mask. Using the brain mask, the minimum and maximum intensities inside the brain are computed and used to normalize the voxel intensities of DSC-MRP images between 0 and 1.

2.3 Regression and Ordinal Regression Tasks

3D-MDRNN conducts two tasks, i.e., the regression task and ordinal regression task. For the regression task, the network aims at predicting a continuous voxel intensity that represents the status of collaterals. As for the ordinal regression task, the objective is to predict the ordinal label per voxel that is indicative of the relative ordering of the collateral status.

The ground truth collateral maps are converted in two separate manners that are tailored for the two tasks. In the regression task, each of the five collateral maps is normalized to a range [-1, 1]. In the ordinal regression task, each collateral map is quantized into a number of disjoint sub-intervals. Formally, each voxel in DSC-MRP is assigned a discrete ordinal value $o \in \{1, \dots, K\}$. K is the cardinality of the ordinal label. We set K to 5. For the discretization of an interval $[\alpha, \beta]$ (We set $\alpha = 0$ and $\beta = 1$), a spacing-increasing discretization strategy (SID) [27] is employed to calculate the threshold values as:

$$t_i = exp\left(\log(\alpha') + \frac{\log\left(\frac{\beta'}{\alpha'}\right) * i}{K} \right), i = 0, \dots, K$$

where $\alpha' = \alpha + \varepsilon$, $\beta' = \beta + \varepsilon$, and $\varepsilon = 0.001$. Using the threshold values, each voxel in DSC-MRP is discretized into K intervals.

2.4 3-D Multitask Deep Regression Neural Network (3D-MDRNN)

The proposed 3D-MDRNN follows an encoder-decoder framework. The computational blocks in the encoder and decoder are built based upon three major components, including densely connected layers [28], residual layers [29], and skip connections. The encoder has one convolution layer and four densely connected blocks. The convolution layer has 8 kernels of size 3 x 3 x 3 (depth x height x width), followed by a max-pooling layer. The densely connected blocks are consisted of 3 x 1 x 1 and 3 x 3 x 3 convolutions that are repeated 6, 12, 24, and 48 times. To reduce the number of output feature maps, each of the four densely connected layers is followed by a transition layer. The number of feature maps of the four densely connected bocks amounts to 32, 64, 128, and 256, respectively.

The decoder exploits residual layers. It includes a 3 x 2 x 2 deconvolution layer to double the height and width of the input feature map and a residual layer with 3 x 1 x 1, 3 x 3 x 3, and 3 x 1 x 1 convolutions. The deconvolution and residual layers are repeated 4 times. The corresponding layers between the encoder and decoder are connected via skip connections. For the prediction, two independent prediction layers are utilized. The first prediction layer uses a 1 x 1 x 1 convolution and a Tanh activation function to predict a continuous intensity in collateral imaging in a range of [-1, 1] (regression). In the second prediction layer, a 1 x 1 x 1 convolution and a Softmax activation function are utilized to predict the discrete ordinal label for collateral imaging (ordinal regression).

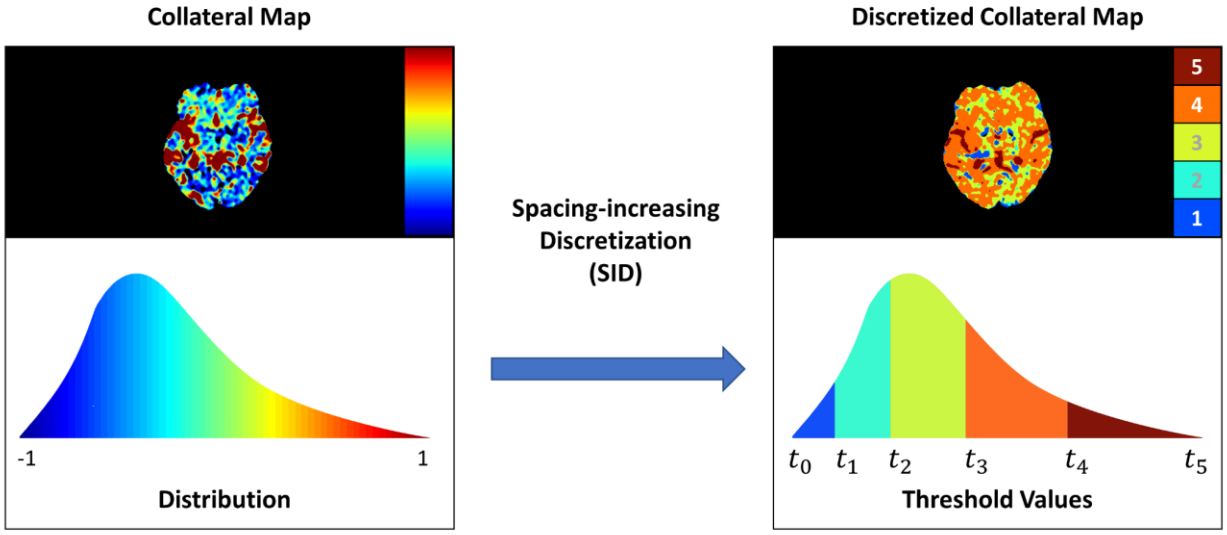

Figure 2. Spacing-increasing discretization (SID) strategy.

2.5 Network training

The proposed network is implemented using the open-source software library PyTorch [30]. It is optimized using ADAM optimizer with parameter $\beta 1 = 0.9$, $\beta 2 = 0.999$, and $\varepsilon = 1e{-}8$. The total loss is calculated as a sum of L2 loss for the regression task and cross entropy loss for the ordinal regression task where a weighting factor for each loss is set to 0.75 (regression) and 0.25 (ordinal regressions), respectively. During training, the following data augmentation is applied for each image: 1) a center crop of size 224 x 224 and 2) a horizontal flip with a probability of 0.5. The 3D-MDRNN is trained for 300 epochs with the initial learning rate is set to 1e–3 and reduced by half after 10 epochs with no improvement. The optimal model is chosen based upon the performance on the validation set, i.e., achieving the lowest validation loss. The chose model is utilized for testing on the test set.

3. RESULTS

Trained on the training set of 205 subjects, the optimal 3D-MDRNN model was selected based upon its performance on the validation set. The optimal model is tested on the test set of 76 subjects. To quantitatively evaluate the performance of the network, the mean, median, standard deviation, minimum, and maximum of R-squared, MAE, TM, and SSIM were computed for each of the five collaterals maps per DSC-MRP image in the test set. On average, the 3D-MDRNN achieved 0.901 R-Squared, 0.063 MAE, 0.945 TM, and 0.933 SSIM. This demonstrates that the proposed method is able to predict the collateral maps with high accuracy. The detailed results of the proposed 3D-MDRNN are shown in Table 1.

The same experiment was repeated for the model without ordinal regression, obtaining 0.882 R-Squared, 0.068 MAE, 0.936 TM, and 0.921 SSIM on average. The experimental results clearly show that the proposed method, equipped with both regression and ordinal regression, outperforms the model without ordinal regression. The superior performance of the proposed method is not dependent on the choice of the evaluation metrics and the collateral phases. These results indicate that the proposed multi-task learning approach, exploiting both regression and ordinal regression, provides a substantial performance gain in predicting collateral maps from DSC-MRP. The details of the comparison experiments are shown in Table 2.

Table 1. Results of collateral imaging prediction.

	R-squared					MAE($x10^{-1}$)				
	Art	Cap	Even	LVen	Del	Art	Cap	Even	LVen	Del
Mean	0.838	0.931	0.920	0.876	0.943	0.680	0.558	0.666	0.744	0.505
Median	0.894	0.943	0.936	0.896	0.951	0.606	0.543	0.604	0.704	0.459
SD	0.140	0.045	0.056	0.071	0.038	0.270	0.135	0.206	0.193	0.129
Min	0.201	0.707	0.663	0.605	0.744	0.313	0.346	0.373	0.456	0.380
Max	0.951	0.966	0.968	0.961	0.973	1.493	0.980	1.601	1.547	0.998
	TM					SSIM				
	Art	Cap	Even	LVen	Del	Art	Cap	Even	LVen	Del
Mean	0.886	0.969	0.960	0.939	0.970	0.879	0.957	0.945	0.922	0.963
Median	0.918	0.974	0.968	0.950	0.976	0.918	0.965	0.956	0.933	0.970
SD	0.086	0.018	0.027	0.032	0.018	0.097	0.026	0.035	0.042	0.023
Min	0.589	0.885	0.823	0.801	0.884	0.458	0.833	0.772	0.771	0.856
Max	0.973	0.987	0.986	0.978	0.986	0.972	0.980	0.976	0.969	0.981

Table 2. Results of comparative experiments.

	R-squared					MAE($x10^{-1}$)				
	Art	Cap	Even	LVen	Del	Art	Cap	Even	LVen	Del
3D-MDRNN	**0.838**	**0.931**	**0.920**	**0.876**	**0.943**	**0.680**	**0.558**	**0.666**	**0.744**	**0.505**
3D-DRNN [21]	0.796	0.912	0.906	0.860	0.937	0.786	0.614	0.669	0.769	0.545
	TM					SSIM				
	Art	Cap	Even	LVen	Del	Art	Cap	Even	LVen	Del
3D-MDRNN	**0.886**	**0.969**	**0.960**	**0.939**	**0.970**	**0.879**	**0.957**	**0.945**	**0.922**	**0.963**
3D-DRNN [21]	0.860	0.963	0.957	0.934	0.968	0.849	0.946	0.940	0.913	0.960

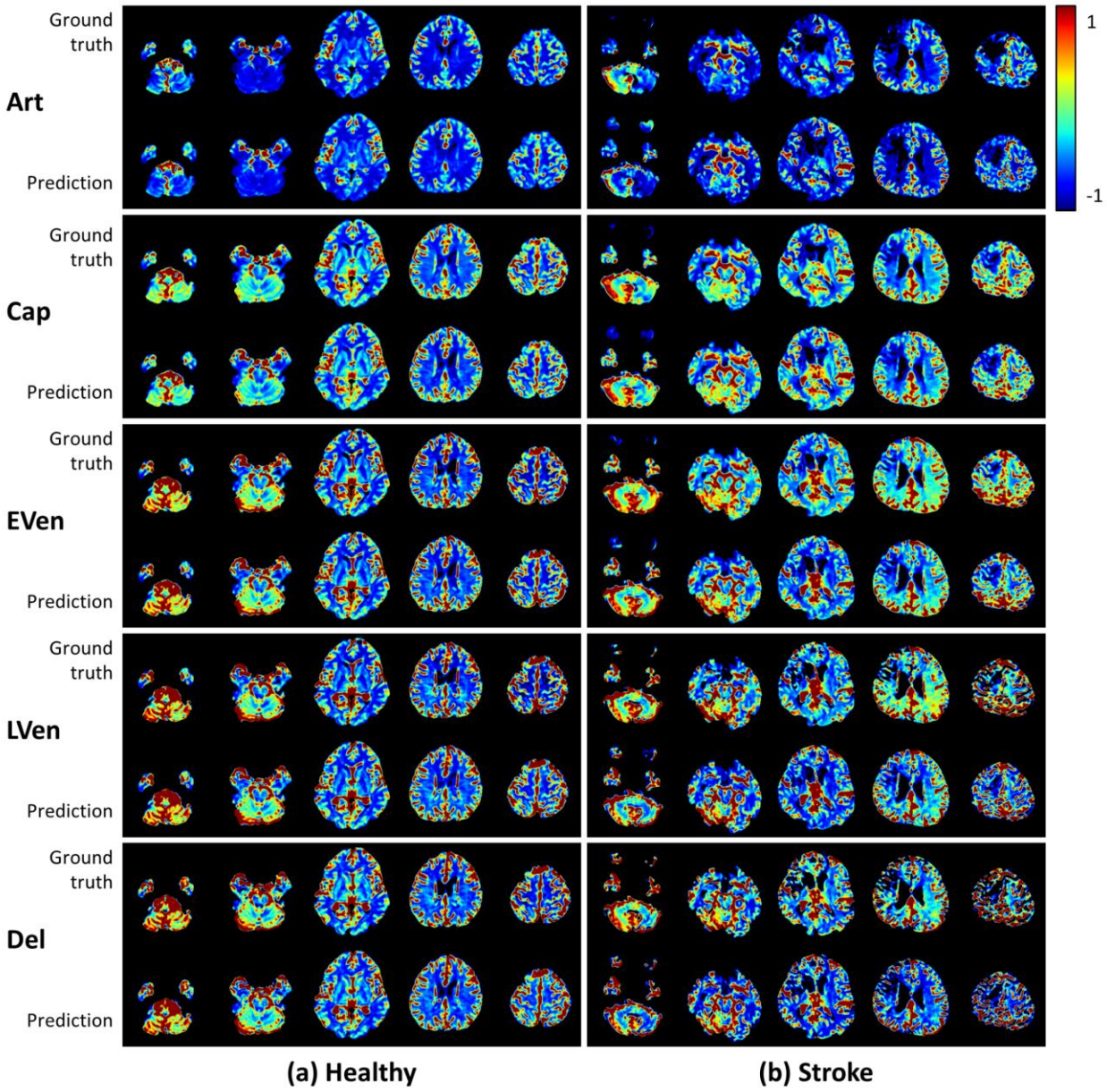

Figure 3. Examples of ground truth and predicted collateral maps for (a) healthy and (b) AIS subjects.

In Art, the prediction power of the proposed 3D-MDRNN was substantially lower than the other four phases. The similar observation was made for 3D-DRNN. In comparison with 3D-DRNN, the higher performance gain was attained from Art than the other four phases. This is may be due to the fact that the overall intensity of Art is lower than the other four phases and deep learning models tend to mis-predict the low intensities in the ground truth collateral maps. The proposed 3D-MDRNN utilizes the SID strategy that concentrates more on the voxels with lower intensities so as to facilitate an improved performance on the low intensity collateral maps, in particular for Art.

Moreover, we visualized the prediction of the proposed network for the five collateral maps, including Art, Cap, Even, LVen, and Del. The five collateral maps of healthy and AIS subjects are provided in Fig. 3. Upon the visual inspection, we found that the proposed 3D-MDRNN is able to accurately generate collateral maps for the five phases that are similar

to the ground truth collateral maps. In the visual comparison between healthy and AIS subjects, no distinctive difference was found with respect to the performance of the proposed 3D-MDRNN.

4. CONCLUSION

In this study, we present a multitask learning approach for collateral imaging in AIS. The prediction of collateral imaging is naturally a regression problem. By adopting the SID strategy, we reformulate it as an ordinal regression problem. Utilizing both regression and ordinal regression learning, the proposed method achieves an improved performance for the prediction of collateral imaging. The proposed method could facilitate an improved assessment and diagnosis of AIS via DSC-MRP.

5. ACKNOWLEDGMENTS

This study was supported by the National Research Foundation of Korea (NRF) grant funded by the Korea government (No. NRF-2020K1A3A1A74114867).

REFERENCES

[1] B. R. French, R. S. Boddepalli, and R. Govindarajan, "Acute ischemic stroke: current status and future directions," Missouri medicine, 113(6), 480 (2016).
[2] D. S. Liebeskind, T. A. Tomsick, L. D. Foster *et al.*, "Collaterals at angiography and outcomes in the Interventional Management of Stroke (IMS) III trial," Stroke, 45(3), 759-764 (2014).
[3] M. Goyal, A. M. Demchuk, B. K. Menon *et al.*, "Randomized assessment of rapid endovascular treatment of ischemic stroke," New England Journal of Medicine, 372(11), 1019-1030 (2015).
[4] O. Y. Bang, J. L. Saver, B. H. Buck *et al.*, "Impact of collateral flow on tissue fate in acute ischaemic stroke," Journal of Neurology, Neurosurgery & Psychiatry, 79(6), 625-629 (2008).
[5] B. K. Menon, C. D. d'Esterre, E. M. Qazi *et al.*, "Multiphase CT angiography: a new tool for the imaging triage of patients with acute ischemic stroke," Radiology, 275(2), 510-520 (2015).
[6] A. García-Tornel, V. Carvalho, S. Boned *et al.*, "Improving the evaluation of collateral circulation by multiphase computed tomography angiography in acute stroke patients treated with endovascular reperfusion therapies," Interventional neurology, 5(3-4), 209-217 (2016).
[7] S. J. Kim, J. P. Son, S. Ryoo *et al.*, "A novel magnetic resonance imaging approach to collateral flow imaging in ischemic stroke," Annals of neurology, 76(3), 356-369 (2014).
[8] H. G. Roh, E. Y. Kim, I. S. Kim *et al.*, "A Novel Collateral Imaging Method Derived from Time-Resolved Dynamic Contrast-Enhanced MR Angiography in Acute Ischemic Stroke: A Pilot Study," AJNR Am J Neuroradiol, 40(6), 946-953 (2019).
[9] H. J. Kim, S. B. Lee, J. W. Choi *et al.*, "Multiphase MR Angiography Collateral Map: Functional Outcome after Acute Anterior Circulation Ischemic Stroke," Radiology, 295(1), 192-201 (2020).
[10] P. M. Robson, W. Dai, A. Shankaranarayanan *et al.*, "Time-resolved vessel-selective digital subtraction MR angiography of the cerebral vasculature with arterial spin labeling," Radiology, 257(2), 507-515 (2010).
[11] Y. LeCun, Y. Bengio, and G. Hinton, "Deep learning," nature, 521(7553), 436-444 (2015).
[12] G. Litjens, T. Kooi, B. E. Bejnordi *et al.*, "A survey on deep learning in medical image analysis," Medical image analysis, 42, 60-88 (2017).
[13] M. P. McBee, O. A. Awan, A. T. Colucci *et al.*, "Deep learning in radiology," Academic radiology, 25(11), 1472-1480 (2018).
[14] A. S. Lundervold, and A. Lundervold, "An overview of deep learning in medical imaging focusing on MRI," Zeitschrift für Medizinische Physik, 29(2), 102-127 (2019).
[15] H. Chen, Q. Dou, L. Yu *et al.*, "VoxResNet: Deep voxelwise residual networks for brain segmentation from 3D MR images," NeuroImage, 170, 446-455 (2018).
[16] X. Zhao, Y. Wu, G. Song *et al.*, "A deep learning model integrating FCNNs and CRFs for brain tumor segmentation," Medical image analysis, 43, 98-111 (2018).

[17] D. Nie, H. Zhang, E. Adeli *et al.*, "3D deep learning for multi-modal imaging-guided survival time prediction of brain tumor patients." 212-220.
[18] L. Chen, P. Bentley, and D. Rueckert, "Fully automatic acute ischemic lesion segmentation in DWI using convolutional neural networks," NeuroImage: Clinical, 15, 633-643 (2017).
[19] A. Pinto, R. Mckinley, V. Alves *et al.*, "Stroke lesion outcome prediction based on MRI imaging combined with clinical information," Frontiers in neurology, 9, 1060 (2018).
[20] Y. Yu, Y. Xie, T. Thamm *et al.*, "Use of Deep Learning to Predict Final Ischemic Stroke Lesions From Initial Magnetic Resonance Imaging," JAMA network open, 3(3), e200772-e200772 (2020).
[21] M. N. N. To, H. J. Kim, H. G. Roh *et al.*, "Deep regression neural networks for collateral imaging from dynamic susceptibility contrast-enhanced magnetic resonance perfusion in acute ischemic stroke," International Journal of Computer Assisted Radiology and Surgery, 15(1), 151-162 (2020).
[22] Y. Zhang, and Q. Yang, "An overview of multi-task learning," National Science Review, 5(1), 30-43 (2017).
[23] S. Mehta, E. Mercan, J. Bartlett *et al.*, "Y-Net: joint segmentation and classification for diagnosis of breast biopsy images." 893-901.
[24] X. Yang, Z. Zeng, S. Y. Yeo *et al.*, "A novel multi-task deep learning model for skin lesion segmentation and classification," arXiv preprint arXiv:1703.01025, (2017).
[25] T. Tanimoto, [An elementary mathematical theory of classification and prediction, IBM Report (November, 1958), cited in: G. Salton, Automatic Information Organization and Retrieval] McGraw-Hill New York, (1968).
[26] Z. Wang, A. C. Bovik, H. R. Sheikh *et al.*, "Image quality assessment: from error visibility to structural similarity," IEEE transactions on image processing, 13(4), 600-612 (2004).
[27] H. Fu, M. Gong, C. Wang *et al.*, "Deep ordinal regression network for monocular depth estimation." 2002-2011.
[28] G. Huang, Z. Liu, L. Van Der Maaten *et al.*, "Densely connected convolutional networks." 4700-4708.
[29] K. He, X. Zhang, S. Ren *et al.*, "Deep residual learning for image recognition." 770-778.
[30] A. Paszke, S. Gross, F. Massa *et al.*, "Pytorch: An imperative style, high-performance deep learning library." 8026-8037.